

## Supporting Information

### Temperature-Induced Switchable Interfacial Interactions on Slippery Surfaces for Controllable Liquid Manipulation

Zubin Wang,<sup>a</sup> Quan Xu,<sup>b</sup> Lili Wang,<sup>a</sup> Liping Heng\*<sup>a</sup> and Lei Jiang<sup>a</sup>

<sup>a</sup>Key Laboratory of Bio-Inspired Smart Interfacial Science and Technology of Ministry of Education, Beijing Key Laboratory of Bio-Inspired Energy Materials and Devices, School of Chemistry, Beihang University, Beijing 100191, China. E-mail: henglp@iccas.ac.cn

<sup>b</sup>State Key Laboratory of Heavy Oil Processing, China University of Petroleum-Beijing, 102249, China

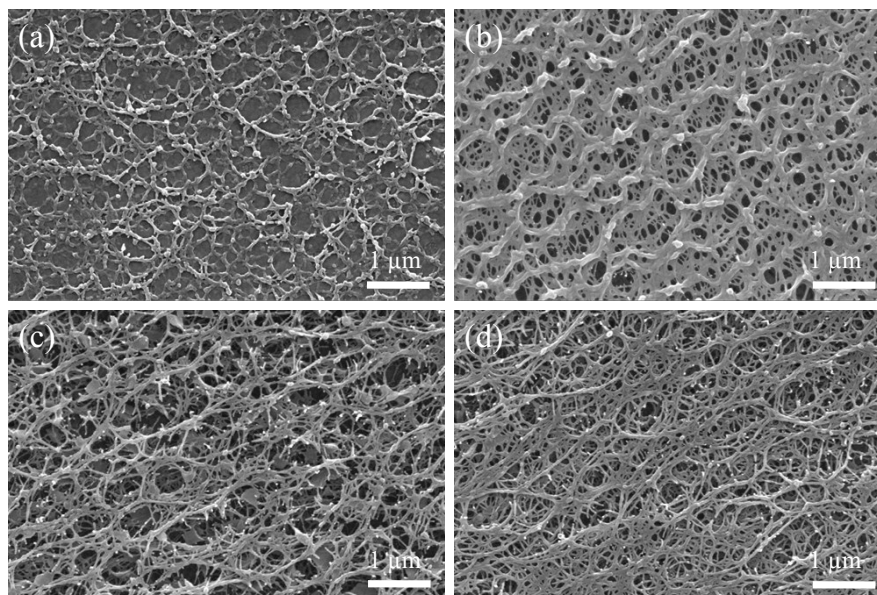


**Fig. S1** SEM images of porous PS films prepared by interfacial freeze-drying using different concentration PS solutions: (a) 1 mg mL<sup>-1</sup>; (b) 2 mg mL<sup>-1</sup>; (c) 3 mg mL<sup>-1</sup>; (d) 4 mg mL<sup>-1</sup>. All the PS films presented a porous structure with pore sizes of 0.2-0.8 μm.

### The effect of droplet density on the droplet sliding behavior:

As shown in **Fig. S2**, when a droplet slides on a tilted slippery surface, the driven force  $F = mg\sin\theta - f = \rho V\sin\theta - f$ , where  $\rho$  and  $V$  indicate the droplet density and volume, respectively. It can be concluded that the dense droplet has the large driven force and therefore small SA, which is good agreement with the measured result (**Fig. 2c** and **Table S1**).

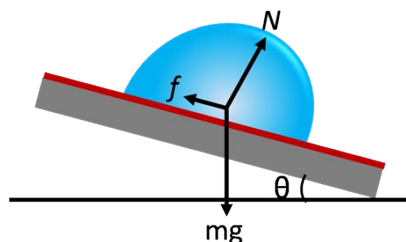


**Fig. S2** The forces loaded on the droplet on a tilted slippery surface.  $N$ ,  $f$  and  $mg$  are the support force, friction force and gravity, respectively.

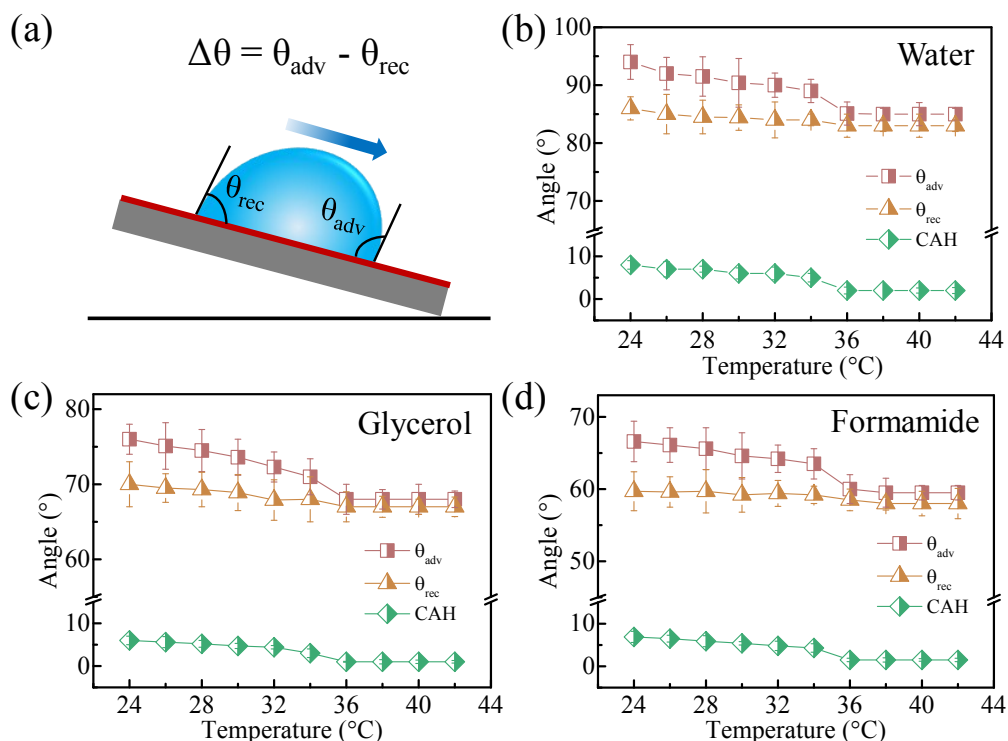


**Fig. S3** (a) The advancing angles and receding angles of a liquid droplet are denoted as  $\theta_{adv}$  and  $\theta_{rec}$ , respectively. The  $\theta_{adv}$ ,  $\theta_{rec}$  and CAH of (b) water, (c) glycerol and (d) formamide on the slippery surface in response to external temperature.

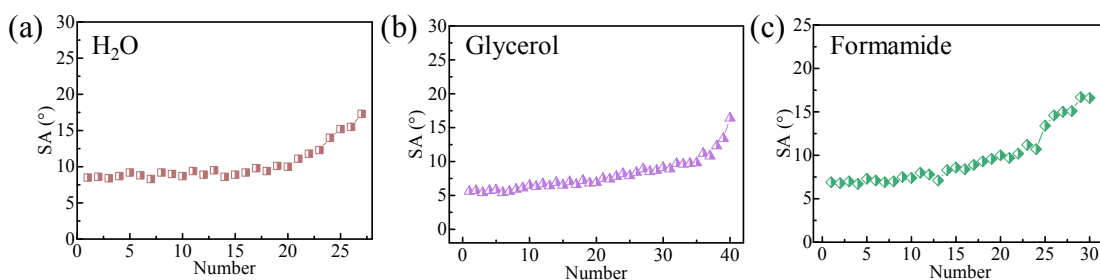


**Fig. S4** The stability of the 5CB infused slippery surfaces. (a) The water SAs increased from 8.5° to 10.0° after dropping 20 droplets and to 17.3° after 27 droplets sliding off the surface. (b) The SAs of glycerol droplets increased from 5.6° to 9.8° after dropping 35 droplets and to 16.4° after 40 droplets sliding off the surface. (c) The SAs of formamide droplets increased from 6.9° to 10.2° after dropping 22 droplets and to 16.6° after 30 droplets sliding off the surface. All test drops slide off the surface along the same path, the temperature used here was 38 °C.

#### **The effect of porous structure of PS film on the stability of slippery surface:**

We used the films obtained from the 1, 3 and 4 mg mL<sup>-1</sup> PS solutions to prepare the slippery surfaces. As shown in Fig. S1, the film obtained from a 1 mg mL<sup>-1</sup> solution showed large areas exposed glass substrate with pore sizes of 0.5-0.8 μm, the film obtained from a 4 mg mL<sup>-1</sup> solution possessed many small pores with sizes of 0.2-0.3 μm and less large pores with sizes of ~ 0.5 μm, and the film prepared from a 3 mg mL<sup>-1</sup> solution had pore sizes of 0.2-0.5 μm. The surface densities of 5CB locked in these porous PS films were measured and indicative of 2.67, 3.55 and 3.15 mg cm<sup>-2</sup>, respectively, showing that porous PS film from 3 mg mL<sup>-1</sup> could lock more 5CB. As shown in Fig. S5, the SAs of water droplets on the above slippery surfaces were measured. It can be found that the slippery surfaces based on the films from 1 and 4 mg mL<sup>-1</sup> solutions show poor stability in comparison with the slippery surface used the film from 3 mg mL<sup>-1</sup> solution. Therefore, the slippery surface based on the PS film from 3 mg mL<sup>-1</sup> solution demonstrates the best stability.

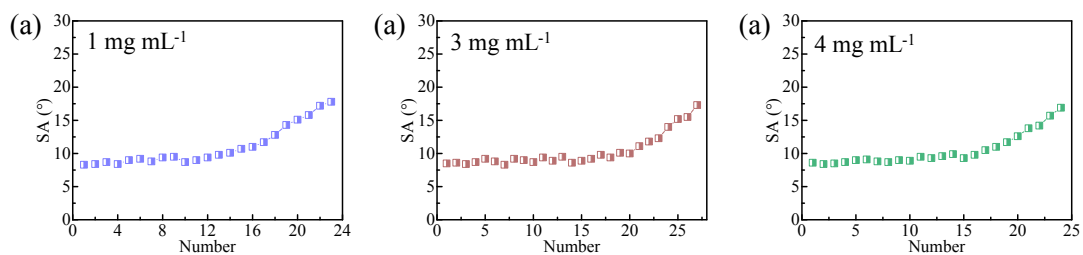


**Fig. S5** The surface stability of slippery surfaces based on the porous PS films from 1, 3 and 4 mg mL<sup>-1</sup> solutions. It can be observed that the slippery surface based on the film from 3 mg mL<sup>-1</sup> solution demonstrated the best stability from the change of water SAs.

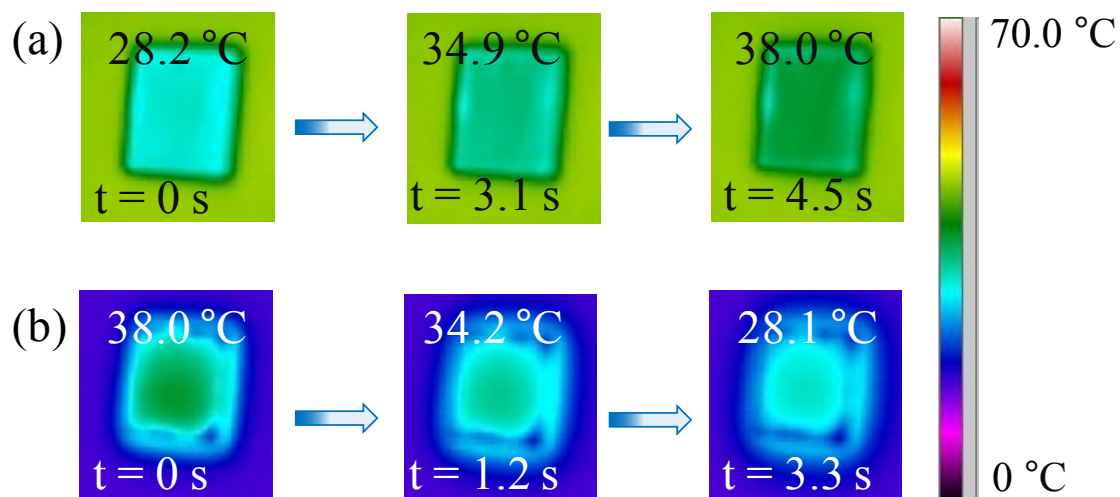


**Fig. S6** The process of (a) increasing and (b) decreasing the slippery surface temperature. It takes 4.5 s to increase the surface temperature from 28.2 to 38.0 °C. In contrast, 3.3 s was needed to decrease the surface temperature from 38.0 to 28.1 °C.

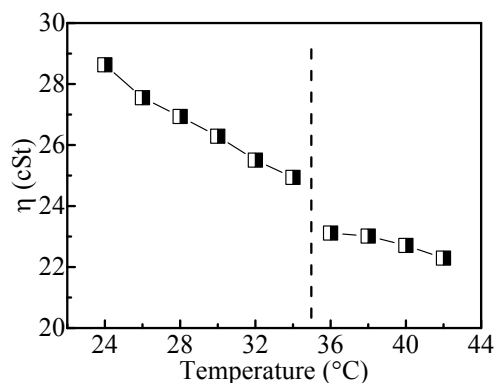


**Fig. S7** Temperature dependence of the viscosity coefficient of 5CB. The dot-dashed line indicates the phase transition temperature. At the phase transition temperature, the viscosity coefficient of 5CB sharply decreases.

### The effect of the change of surface tension on the liquid SA.

To verify the effect of the change of 5CB surface tension on liquid SA, another slippery surface was prepared using a lubricant without temperature-responsiveness and the same porous PS film. As shown in **Fig. S8a**, the surface tension of the lubricant (ionic liquid, 1-octyl-3-methylimidazolium tetrafluoroborate, [OMIm][BF<sub>4</sub>]) decreased from 31.3 to 28.5 mN m<sup>-1</sup> as the temperature was increased from 24 to 42 °C. When the temperature was heated from 24 to 42 °C, the water SAs on such slippery surface kept at ~3.0° (**Fig. S8b**), showing that the small change of lubricant surface tension has no obvious effect on liquid SA.

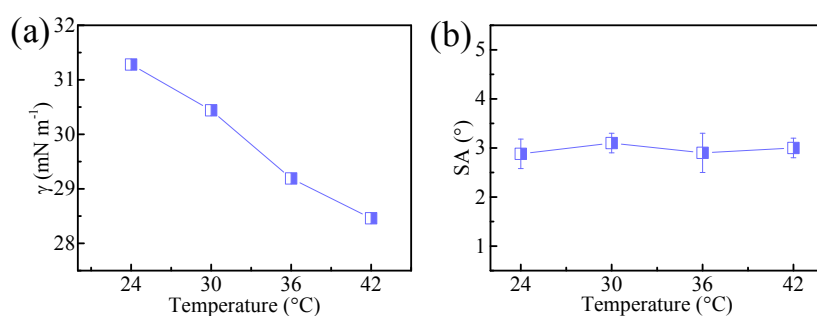


**Fig. S8** (a) The surface tension of the ionic liquid ([OMIm][BF<sub>4</sub>]) as a function of temperature. (b) Water SA on the ionic liquid-infused surface in response to the increasing external temperature.

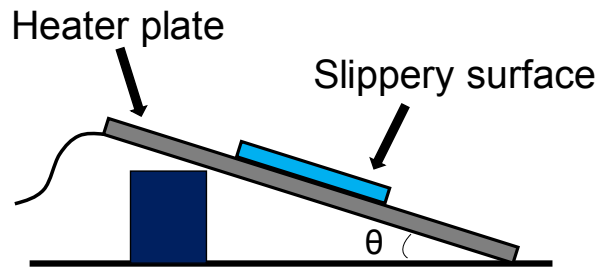


**Fig. S9** The Schematic side-view of the slippery surface on the heater plate.

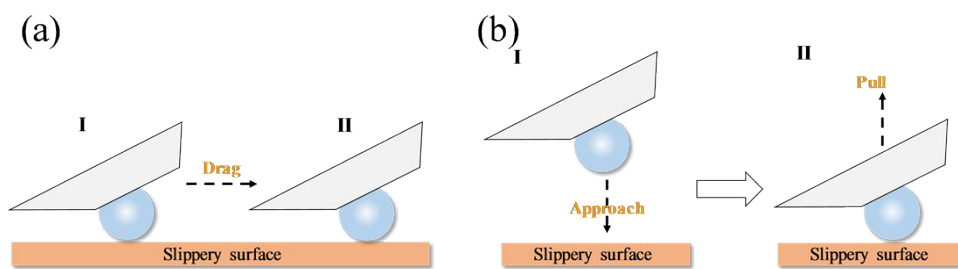


**Fig. S10** Scheme of the (a) friction force and (b) adhesion force measurements.

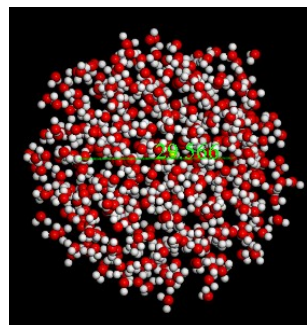


**Fig. S11** The water droplets with diameter of 3 nm used in the simulation process.

**Table S1** Surface tension ( $\gamma$ ) at 24 and 42 °C, viscosity and density of different liquid.

<b>Liquid</b>	$\gamma$ (mN m <sup>-1</sup> , 24 °C)	$\gamma$ (mN m <sup>-1</sup> , 42 °C)	<b>Viscosity</b> (cSt)	<b>Density</b> (g cm <sup>-3</sup> )
Water	72.1	69.3	0.89	1.00
Glycerol	62.7	60.7	559.30	1.26
Formamide	57.4	55.9	2.03	1.13
5CB	34.6	32.3	28.6	1.008

**Table S2** The surface tension of droplet ( $\gamma_d$ ), 5CB ( $\gamma_l$ ), and interfacial tension ( $\gamma_{dl}$ ) between droplet and 5CB, and CAs of droplets ( $\theta_d$ ) and 5CB ( $\theta_l$ ) on the porous PS film and the calculated  $\Delta E$  at 24 °C.

<b>Droplet</b>	$\gamma_d$ (mN m <sup>-1</sup> )	$\gamma_l$ (mN m <sup>-1</sup> )	$\gamma_{dl}$ (mN m <sup>-1</sup> )	$\theta_d$	$\theta_l$	$\Delta E$
Water	72.1	34.6	31.6	112°	16°	28.7
Glycerol	62.7	34.6	21.1	100°	16°	23.0
Formamide	57.4	34.6	14.1	87°	16°	16.2

**Table S3.** The surface tension of droplet ( $\gamma_d$ ), 5CB ( $\gamma_l$ ), and interfacial tension ( $\gamma_{dl}$ ) between droplet and 5CB, and CAs of droplets ( $\theta_d$ ) and 5CB ( $\theta_l$ ) on the porous PS film and the calculated  $\Delta E$  at 38 °C.

<b>Droplet</b>	$\gamma_d$ (mN m <sup>-1</sup> )	$\gamma_l$ (mN m <sup>-1</sup> )	$\gamma_{dl}$ (mN m <sup>-1</sup> )	$\theta_d$	$\theta_l$	$\Delta E$
Water	69.9	32.7	29.7	103°	11°	18.1
Glycerol	61.1	32.7	19.0	90°	11°	13.1
Formamide	56.2	32.7	12.6	79°	11°	8.8